Optical Double Resonance and Level Crossing Spectroscopy under Pulsed Laser Excitation

Diploma Paper by
Jörgen Larsson

Department of Physics

LRAP-81
1987

CONTENTS

Acknowledgements

I would like to thank a number of persons for contributing to this diploma work. My supervisor Prof. Sune Svanberg has provided help and encouragement. Lennart Sturesson made a substantial contribution to the experimental part. Lars Gramstad provided invaluable help in making the old Göteborg programs run on the Lund computers.

Introduction

Optical Double Resonance (ODR) and Level Crossing spectroscopy (LC) are two closely related high-resolution techniques.

ODR was suggested by Kastler and Brossel in 1949 [1]. Two years later Brossel and Bitter demonstrated the technique on the resonance line of mercury [2].

The theory of LC is based on the Breit formula from 1933 [3], but already in 1924 Hanle studied zero-field crossings in mercury [4]. In 1959 Colgrove et al. studied fine-structure, high-field crossings in ^{4}He [5]. Two years later Franken further developed the theory of resonance scattering [6].

ODR and LC are primarily used to investigate atomic hyperfine and small fine structures. Using these techniques, it is possible to determine the magnetic dipole interaction constant and the electric quadropole interaction constant also denoted as a and b factors. In ODR, Lande' or g_J-factors can be determined as well. From the effect of an external electric field the tensor polarizability, α_2 can be evaluated. Since resonance phenomena occurring in individual atoms are used, neither scalar polarizabilities, α_0 nor isotopic shifts can be measured.

The two techniques are both essentially Doppler-free. In ODR Doppler broadening is eliminated since the transitions are induced by a radio-frequency field. Typical RF frequencies are 10^6 to 10^8 times less than those of visible light. Thus the Doppler width is reduced by the same factor. LC is a coherence phenomenon, by definition Doppler-free. To achieve this high resolution no narrow-band lasers are required, since the laser is used only to populate the state to be examined. The first experiments were carried out with RF lamps. The Breit formula for LC, in fact, demands broad-banded ("white") excitation.

Many spectroscopic techniques require CW-lasers operating in a single mode [7]. These lasers operate in a rather limited wavelength region. Single-mode lasers that operate at extreme wavelengths are when obtainable very expensive. At these wavelengths, lasers are often pulsed and broadbanded, but with high peak spectral power. It would be attractive to combine the advantages of theese pulsed lasers with the ODR and LC methods.

One high-resolution technique, employing pulsed lasers, which is frequently used is Quantum Beat (QB) Spectroscopy. QB and LC are closely related. LC is in fact the time integral of the QB-signal. However, QB demands fast time-resolving electronic units. These are often expensive so pulsed ODR and LC may be a good alternative, even when the QB method in principle is possible. ODR has the further advantage that cascade detection can be used. This can be very useful

in eliminating background light. Furthermore, by inducing RF transitions in the intermediate states populated in the cascade decay, these can be studied. In LC the Hanle signal can be detected in cascade light. The high-field crossings, however, cannot be seen, since the coherence is washed out.

This diploma work includes both a theoretic and a experimental description of LC and ODR. The experimental part is devided into three parts, each describing different ways of excitation. First multi mode, then single mode and finally pulsed excitation. In each part results for both LC and ODR are presented. After a brief description of computer programms a discussion on possible pulsed excitation set-ups is carried out.

Theory

In ODR by choice of geometry and polarization the atoms seen as electric dipoles are oriented either parallel (π-excitation, $\Delta m=0$) or perpendicular (σ-excitation, $\Delta m=\pm 1$) to the magnetic field. The scattered light then has a certain distribution. By applying an RF field, the orientation is destroyed and the scattered light is redistributed, of course leaving the total intensity unaltered.

The more accurate theory of ODR is based on the Majorana-Rabi formula [8],[9]. This formula states the transition probability P(F,m,m',t), between levels with magnetic quantum number m and m' at total angular momentum F and time t. It is derived from the time-dependent Schrödinger equation and therefore is valid for large RF amplitudes and large values of time. The interpretation in the Zeeman region is straight forward. In this diploma work the experiments were carried out in the Paschen-Back region inducing transitions $\Delta m_J=\pm 1$ $\Delta m_I=0$.

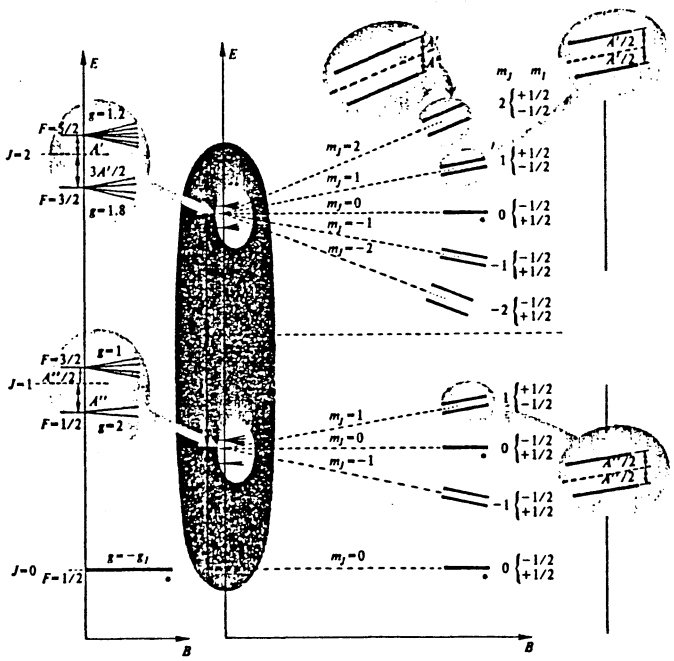

Fig. 1 Influence of magnetic field on atomic states (From [10].)

The transitions are essentially the same as between fine structure Zeeman levels and the Majorana-Rabi formula can be stated as

$$P(J,m,m',t)= \{\cos(v/2)\}^{4J}\cdot(J+m)!(J+m')!(J-m)!(J-m')!\cdot$$

$$\left[\sum_{n=0}^{2J} \frac{(-1)^n \{\tan(v/2)\}^{2n-m+m'}}{n!(n-m+m')!(J+m-n)!(J-m'-n)!}\right]^2 \qquad (1.1)$$

v is an angle defined by

$$\sin^2(v/2)= \frac{(\omega/\gamma H)^2}{1+\{1+(H_z/H)\}^2}\cdot \frac{(\gamma H)^2}{(\gamma H)^2+(\omega-\omega_0)^2}\cdot\sin\left[1/2\{(\gamma H)^2+(\omega-\omega_0)^2\}^{0.5}\, t\right] \qquad (1.2)$$

where H_z is the magnetic field giving rise to the magnetic splittings and H is amplitude of the oscillating field, and ω its angular frequency. The quanity ω_0 is given by

$$\omega_0=g_J\mu_B H_z/\hbar \qquad (1.3)$$

If H is small compared to H_z ($H/H_z<1/10$) the following approximation can be made

$$\sin^2(v/2)=\frac{(\gamma H)^2}{(\gamma H)^2+(\omega-\omega_0)^2}\cdot\sin\left[1/2\{(\gamma H)^2+(\omega-\omega_0)^2\}^{0.5}t\right] \qquad (1.4)$$

Electrons, are excited from m to μ, transfered to μ', by the RF field. Finally , they decay to m'. This is the signal we detect. The intensity of this light is equal to

$$N_{\mu'}{}^*A_{\mu'm'} \qquad (1.5)$$

where $A_{\mu'm'}$ is the transition probability between μ' and m'. μ and μ' designate excited states, while ground states are designated by m or m'. $N_{\mu'}$ is the total number of excited atoms in the sublevel μ' given by the integral

$$\int_0^\infty nP(J,\mu,\mu',t)*\exp(-t/\tau)dt \qquad (1.6)$$

where τ is the lifetime of the excited state and n is the number of photons absorbed per time unit. If steady state conditions can be assumed

$$n=N_{\mu}/\tau \tag{1.7}$$

$$N_{\mu}=A_{\mu m}*N_{m}*I \tag{1.8}$$

where I is the intensity of the exciting light, $A_{\mu m}$ is the transition probability and N_m is the number of atoms in the ground state. In this work the frequency was held constant as the magnetic field was swept. This of course corresponds to sweeping ω_0.

Thus 2I+1 peaks with centre of gravity at

$$B=\omega\hbar/g_J\mu_B \tag{1.9}$$

with a separation giving information about a and b.

If the integral (1.6) is carried out for small RF amplitudes a bell-shaped signal will be found. The width at half maximum is $1/(\pi\tau)$. For larger amplitudes the signal will become wider approximately linear to the square of the RF amplitude (Fig. 2). At even larger amplitudes it becomes distorted (Fig .3).

In this diploma work experiments with delayed detection were carried out. By detecting a sub-group of atoms, which have survived longer than at average, a sub-natural resolution can be achieved. However, as the peak is narrowed oscillations occur in the flanks. ODR experiments at sub-natural resolution was first performed by Ma et al. in 1968 [11].

A good revue of sub-natural resulution techniques, has been given by O'Brien et al. [12].

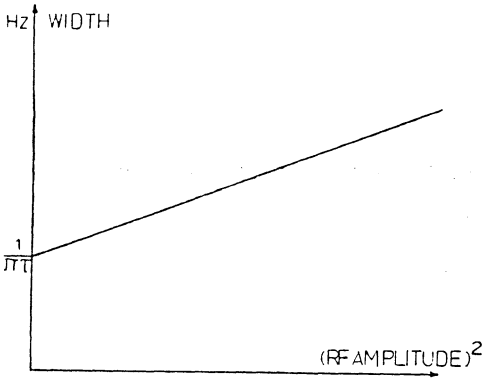

Fig.2 Width of ODR signal for increasing RF amplitude

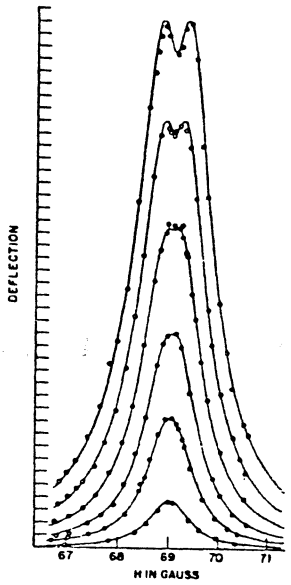

Fig.3 Lineshape of ODR signal for increasing amplitude (From [2].)

LC is a phenomenon which can be studied in the fluorescence light of coherently excited states. In intermediate fields, levels with different angular and magnetic quantum numbers (μ μ') can cross (Fig. 4).

Consider two levels in the upper state with magnetic quantum numbers μ and μ' differing by two units and a level in the lower state with quantum number m differing from the two upper levels by one (Fig. 5). σ-transitions are allowed to both states. In the region where an energy overlap exist, due to the Heisenberg uncertainty relation, a coherent excitation is possible. The absorption cross-section is not altered as the levels cross, only the angular distribution of the scattered light is affected. When the levels are completely resolved the scattered intensity (S) is given by

$$S=\text{Const}\cdot|f_{m\mu}\cdot g_{\mu m}|^2+|f_{m\mu'}\cdot g_{\mu' m}|^2 \qquad (1.10)$$

and when completely unresolved

$$S=\text{Const}\cdot|f_{m\mu}\cdot g_{\mu m}+f_{m\mu'}\cdot g_{\mu' m}|^2 \qquad (1.11)$$

$$f_{m\mu}=\langle m|\underline{f}.\underline{r}|M\rangle \qquad (1.12)$$

$\underline{f}$ is the polarization vector for the exciting light and $\underline{g}$ is the one for the detected light.

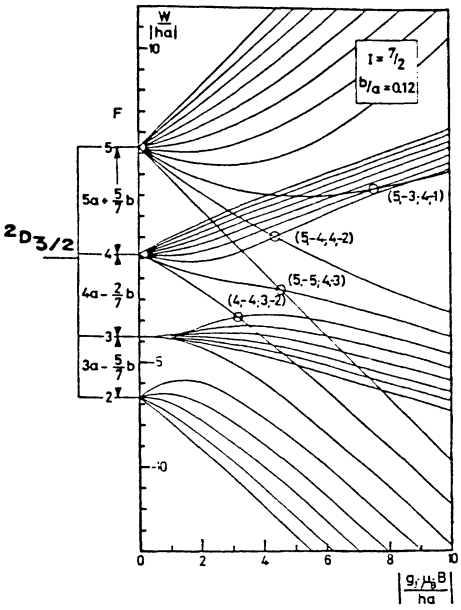

Fig. 4 Energy-level diagram for a $^2D_{3/2}$ *state in* ^{133}Cs *(From [13]).*

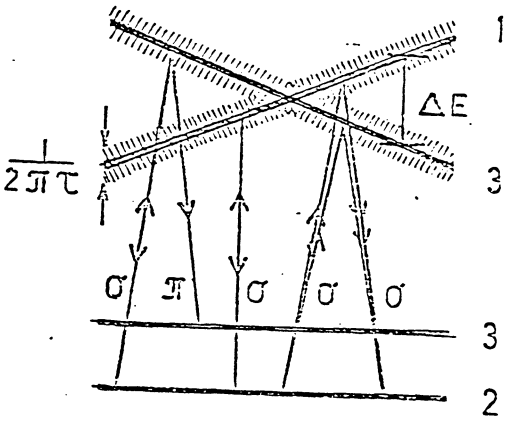

Fig. 5 The principle of LC (From [14]).

In the area in between these two extreme cases a more complex formula is valid. The general expression is the Breit formula yielding

$$S = C \cdot \sum_{\mu\mu'} \sum_{mm'} \frac{f_{\mu m} \cdot f_{m\mu'} \cdot g_{\mu' m'} \cdot g_{m'\mu}}{1 + 2i \cdot \pi \cdot \tau \cdot \nu_{\mu\mu'}} \qquad (1.13)$$

τ is the excited state lifetime. $\nu_{\mu\mu'}$ is the frequency separation between the excited state magnetic sublevels.

This general formula is valid for all geometries and for both $\Delta m=2$ crossings as described above and $\Delta m=1$ crossings

A derivation of the Breit formula has been given by Franken [6] and is carried out in Appendix 1. In [14], (1.13) is rewritten as

$$S = C \cdot \sum_{\mu\mu'} \sum_{mm'} \frac{\mathrm{Re}[K_{\mu\mu'}] + 2 \cdot \pi \cdot \tau \cdot \nu_{\mu\mu'} \cdot \mathrm{Im}[K_{\mu\mu'}]}{1 + 4 \cdot \pi^2 \cdot \tau^2 \cdot \nu^2_{\mu\mu'}} \qquad (1.14)$$

$K_{\mu\mu'}$ is defined as

$$K_{\mu\mu'} = \sum_{mm'} f_{\mu m} \cdot f_{m\mu'} \cdot g_{\mu' m'} \cdot g_{m'\mu} \qquad (1.15)$$

In Appendix 2 this formula is evaluated for the geometry used in the experiments. The lineshape for the signal is a Lorenzian when light polarized parallel to the x- or y-axes is detected. At 45 degrees to the axes a dispersion curve occurs.

As mentioned earlier LC is the time integral of QB. QB is an interference phenomenon involving several wavefunctions. Two or more levels are excited by the same photon, either from a broad laser (short pulse times) or at a level crossing. Superimposed upon the decay curve are oscillations of a frequency corresponding to the energy separation between the levels.

Consider a case where light, polarized perpendicular or parallel to the polarization vector of the exciting light, is detected. Quantum beats between an upper state consisting of two levels and a single level lower state is studied (Fig. 6). The expression for the quantum beats is given in (1.16).

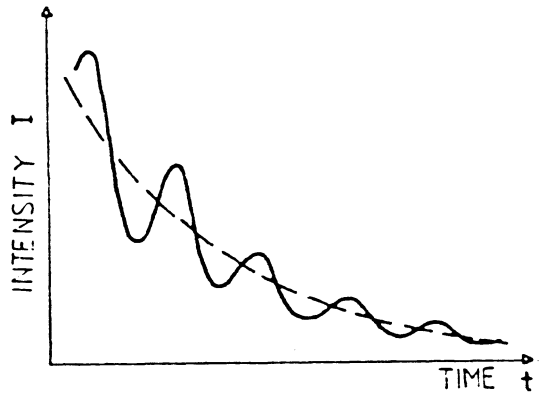

$$I(t)=Ae^{-t/\tau}(1+B\cos\omega t)$$

Fig. 6 The principle of QBS (From [14])

$$I(t)=A\cdot e^{-t/\tau}\cdot(1+B\cos(\omega t)) \qquad (1.16)$$

The level crossing signal is the time integral of the QB signal. When performing this intergral a standard integral is found. The result is

$$S=Const\cdot\left[B\cdot\frac{\omega t\cdot\sin\omega t-\cos\omega t}{1+\omega^2\tau^2}-\frac{e^{-t/\tau}}{\tau}\right]_d^{\infty} \qquad (1.17)$$

For the lower limit d=0 the usual Lorenzian is found, but when introducing delayed detection an oscillating function whose cental peak is narrowed compared to the Lorenzian is found. (Fig. 7). In 1968 the first sub-natural resolution LC experiments were carried out by Copley et al [15].

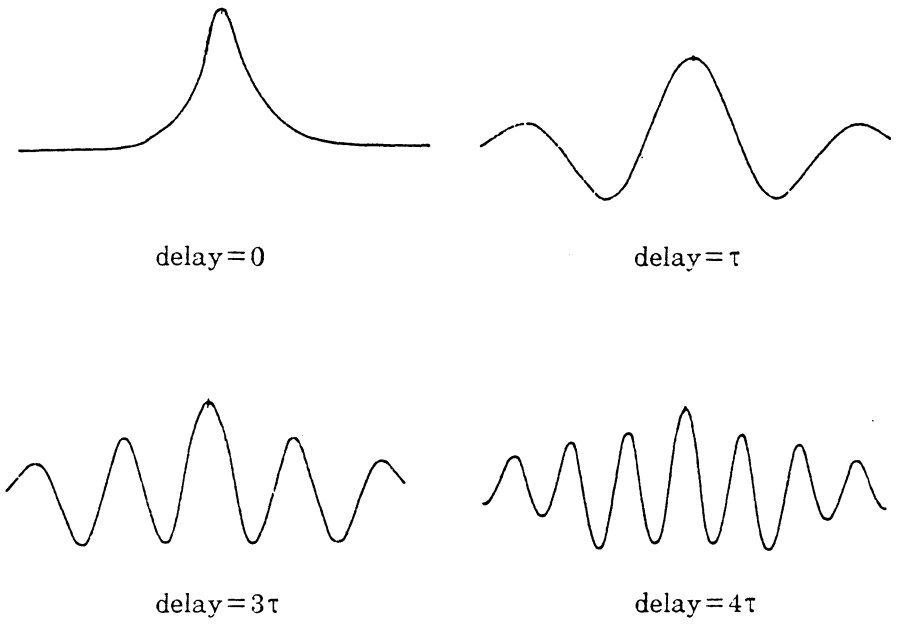

Fig. 7 Theoretical LC-signals for various delay times (adapted from [16])

Experiments.

The techniques were investigated by studying ^2D states in Cs and Rb. These states were first studied using ODR and LC in 1973 [13] The sample atoms were contained in cells. The experimental set-up is shown in Fig. 8

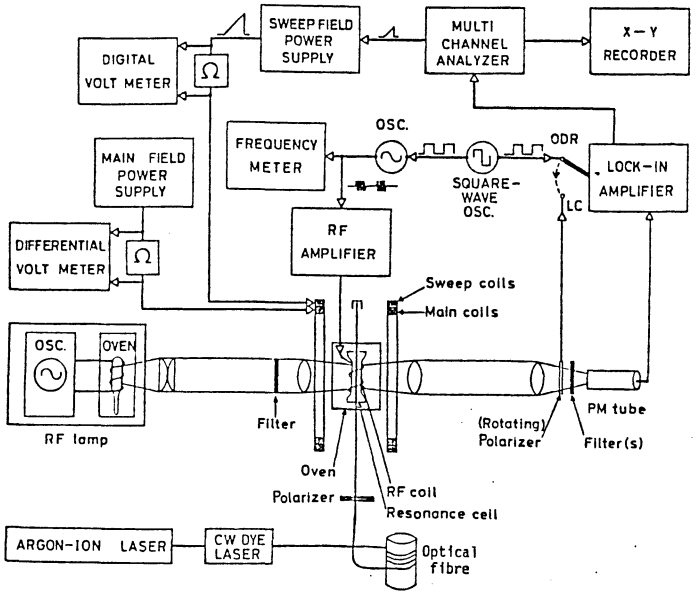

Fig. 8 Experimental set-up

To populate the ^2D states two step excitation from the $6^2S_{1/2}$ ground state was used.

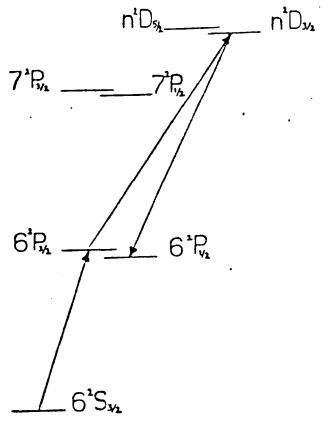

n	λ_1	λ_2
8	6218	6010
9	5848	5664

Fig. 9 Example of two-step excitation of $^2D_{3/2}$ levels in ^{133}Cs

The first state was populated with an RF lamp. A cut off filter was placed between the lamp and the sample cell to make sure that only the resonance line was transmitted. The lamp cells were manufactured at this department. A description of the procedure is made in Appendix 2. Two different Ar^+-ion laser pumped dye lasers were used in different experiments. At first a Coherent 599 unit operating in multimode, was used to achieve white excitation. At a later stage a Coherent 699 single-mode ring laser was employed.

The exciting laser light was sent through an optical fibre instead of using mirrors. This was convenient for security reasons and for avoiding disturbanses. The intensity loss over 100 metres of fibre was about 50%, including input/output losses. Furthermore the polarisation was completely lost, calling for a polarizer to be inserted. The useful power of the light was reduced to approximately one fifth. This should be compared to the use of three mirrors with 90% reflectance, introction of a beam expander, a polarization rotator and an aperture. In such a case about half the power is lost.

The sample cell containing ^{133}Cs was heated by hot air to 90-95 ^{0}C. The magnetic field was produced by two pairs of Helmholz coils, one for sweeping the field while the other was used to give a desired offset. Since the apparatus was set up in the north-south direction only compensation of the vertical component of the Earth magnetic field was necessary. RF transitions were induced by a coil wired around the cell and connected to a RF oscillator and an amplifier. For detection a EMI 9558 Photo multiplyer tube (PMT) was employed. The filters used on the detection side was a combinaton of a coloured-glass filter and an interference filter.

To improve the signal to noise (S/N) ratio, Lock-in techniques were applied. In the LC experiments, where for obvious reasons σ-excitation always was used, a rotating polarizer was put on the detection side. This was rotated at approximately 19 Hz. As shown in Appendix 2, when the polarizer is turned 90 degrees the signal is inverted. Hence a 38 Hz modulation over two times the signal is achieved (Fig. 10a). In an alternative set-up using coils for modulating the magnetic field, modulation is made over a small part of the signal. (Fig. 10b) On the other hand, much higher modulation frequencies can be used. In this diploma work rotating polarizer modulation was used. To further improve the S/N ratio a Tracor signal averager was used to add several sweeps of the magnetic field.

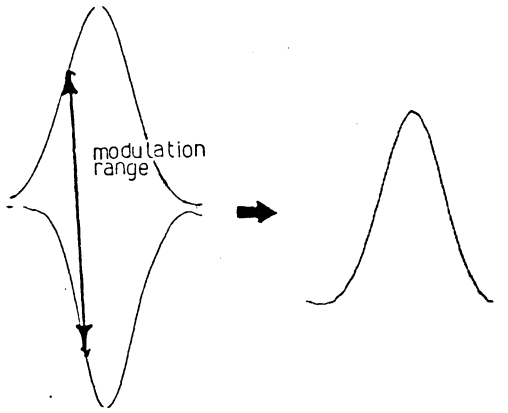

Fig. 10a Rotating polarizer

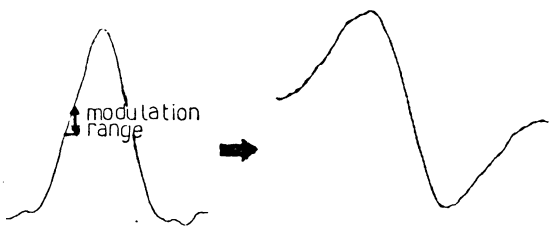

Fig. 10b Modulation with field coils

In ODR π- or σ-excitation can be used. The one resulting in the best signal to background ratio should be used. A simple way is of course to examine this experimentally. It is, however, possible to calculate the signal to background ratio theoretically assuming RF saturation knowing the matrix elements of the electric dipole operator [17].

The excitation to the 8^2D states was carried out using the multimode laser with Rhodamine B dye. The $8^2D_{3/2}$ state was studied with LC technique. Because of the mode structure, "white" excitation is not completely achieved. The modes are unstable and the output power is low (150mW), therefore the signal is quite noisy (Fig. 11). To better acomplish "white" excitation it is possible to connect the output of a sinus wave generator, operating at kHz frequencies, to the tweeter. The tweeter is usually used to stabilize modes in single mode operation. As this is done the modes move back and forth much faster than the lock-in frequency, and a situation resembling "white" excitation is achieved.

The filter between the lamp and the cell was a 3mm thick 7800 A cut-off filter. On the detection side a 6000 Å interference filter was used in combination with a 2 mm thick BG 18 Schott coloured-glass filter.

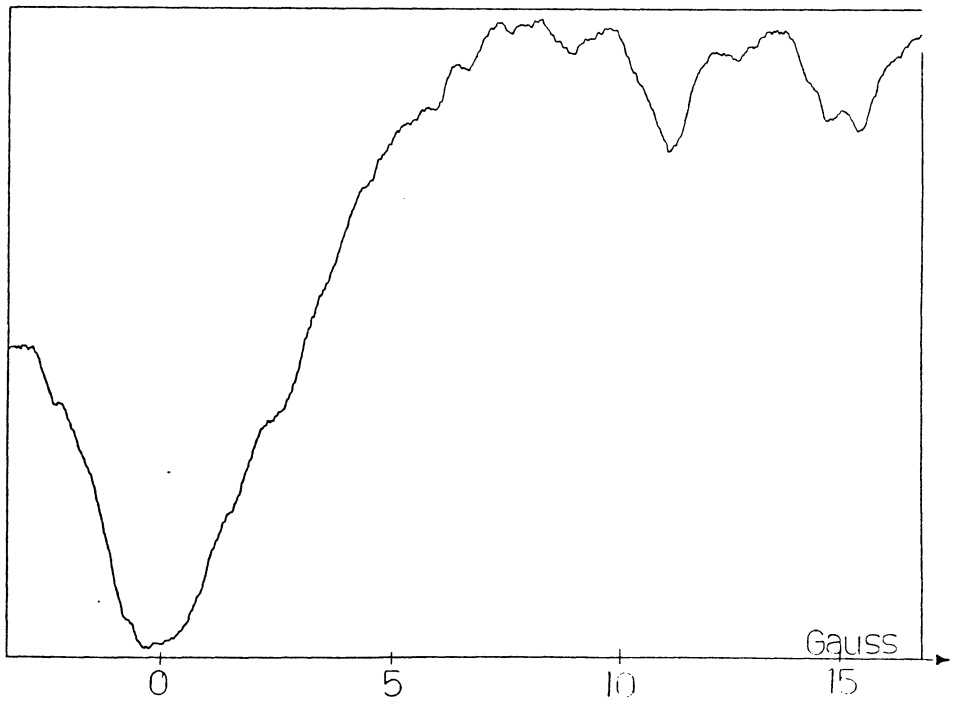

Fig. 11 LC plot for $8^2D_{3/2}$ in ^{133}Cs

For the $8^2D_{3/2}$ state, excitation and detection could be carried out at two different wavelengths, since both the $6^2P_{3/2}$ and the $6^2P_{1/2}$ level can communicate with both the ground and the excited states. (Fig. 9)

In cell experiments this is esssential, as the laser light scattered in glass surfaces will dominate over the flourescent signal. For the $8^2D_{5/2}$ state only the $^2P_{3/2}$ states connect the ground and excited state. As the transition between the $8^2D_{5/2}$ and the $7^2P_{3/2}$ levels is in the infrared region, where background light cannot be surpressed

the only remaining alternative is cascade detection, using the $7^2P_{3/2}$ to $6^2S_{1/2}$ transition. As cascade detection is not possible in LC, ODR was used. Lock-in technique was applied and the RF-field was modulated at 39 Hz. A 458 nm interference filter was used on the detection side.

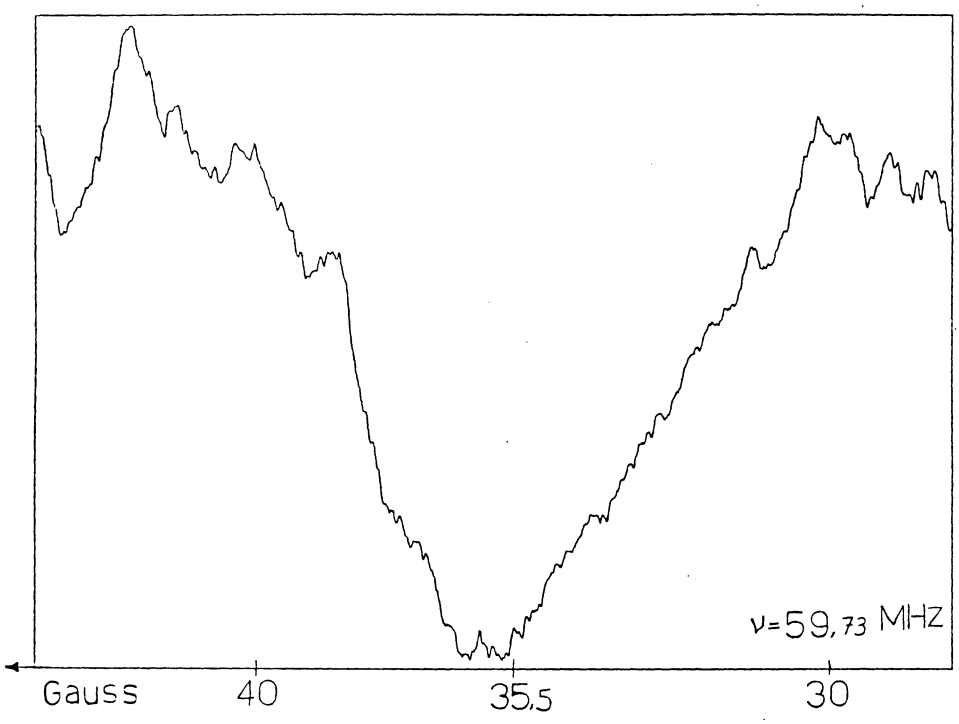

Fig. 12 ODR signal for $8^2D_{5/2}$ in ^{133}Cs

The 9D states were populated with a single-mode laser. Detection was made through a 573 nm interference filter held at an angle to achieve maximum transmition at the desired 566 nm. A 3 mm thick BG 18 filter was inserted to further surpress background light. The $9^2D_{3/2}$ state was studied with LC. The theoretical Doppler linewidth for transitions between the excited and the intermediate state is about 600 MHz. The hyperfine structure is approximately 20 MHz(a=2.37 MHz [13]) and the linewidth of the laser 1 MHz. The excitation is far from white and the Breit formula is obviously not valid. For the intermediate $6^2P_{3/2}$ state the hypefine structure (hfs) is about 600-700 MHz (a=50,31 MHz, b=-0.30 [18]) and depending on where in the Doppler profile the exciting light is situated, different hyperfine groups are of different significance. The selection rules cause that this weighting of hfs levels is transferred to the $^2D_{3/2}$ state. Calculating transition probabilities in the intermediate region is not trivial and a complete interpretation of the resulting curves given in Fig. 14a-14g is beyond the scope of this diploma work. The width and positions of the high field crossings is not altered and the same quantities as in "white" excitation LC can be determined.

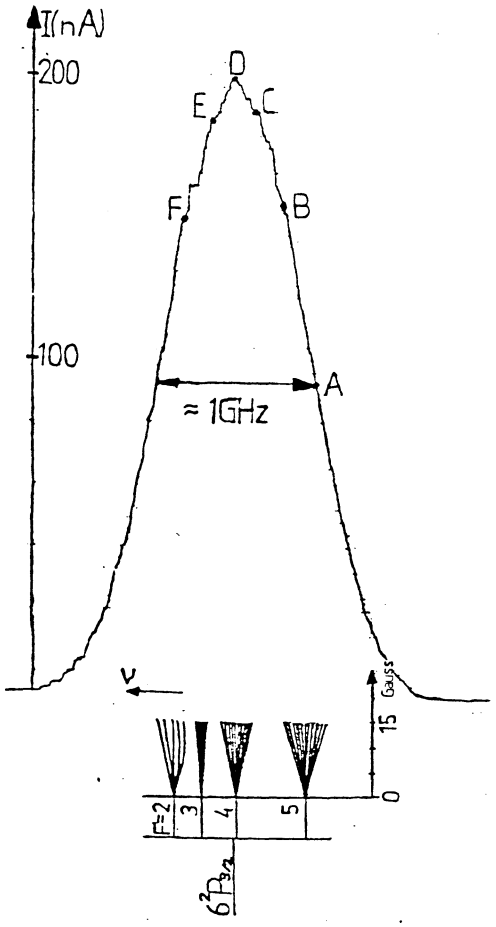

Fig. 13 Dopplerprofile for the transitions between the $6^2P_{3/2}$ and $9^2D_{3/2}$ states and hyperfine structure for the $6^2P_{3/2}$ state

Since the width of the Hanle signal depend on the g_F factor and its amplitude alter significantely depending on which hyperfine group is of most importance, strong modifications of the LC-signal can be seen in Fig. 14. The g_F factors and the Hanle amplitudes are listed in Tab. 1 .

F	g_F	Normalized Hanle Ampltude
2	-0.5	0.041
3	0	0.333
4	0.2	0.081
5	0.3	0.545

Tab. 1

It is obvious that the F=5 and the F=3 signals are the dominant ones. In a simple Zeeman approximation, the width of the Hanle signal is reversely proportonal to the g_F-factor. As $g_F(F=3)=0$ the width for this signal instead is determined by decoupling. In the experiments it can be seen that the Hanle signal gets wider as the importance of the F=3 sub-state is increased. (Compare to the computer read-outs from the Hanle program described in Part 4). (Fig. 15a-15g) Since the computer program uses a Zeeman approximation and the g_F factor is zero, the F=3 signal is infinitely wide. The presence of this coherence is seen as an offset to the signal.

As the F=5 and F=4 states are strongly illuminated the second two overlapping level crossings involving Zeeman substates from these are the dominant ones. As the laser wavelength is altered towards the F=3 and F=2 states, the first level crossing become larger compared to the sum of the two others. The influence of the illumination profile, on the width of the Hanle signal in some states in ^{209}Bi has been studied by Svanberg [19].

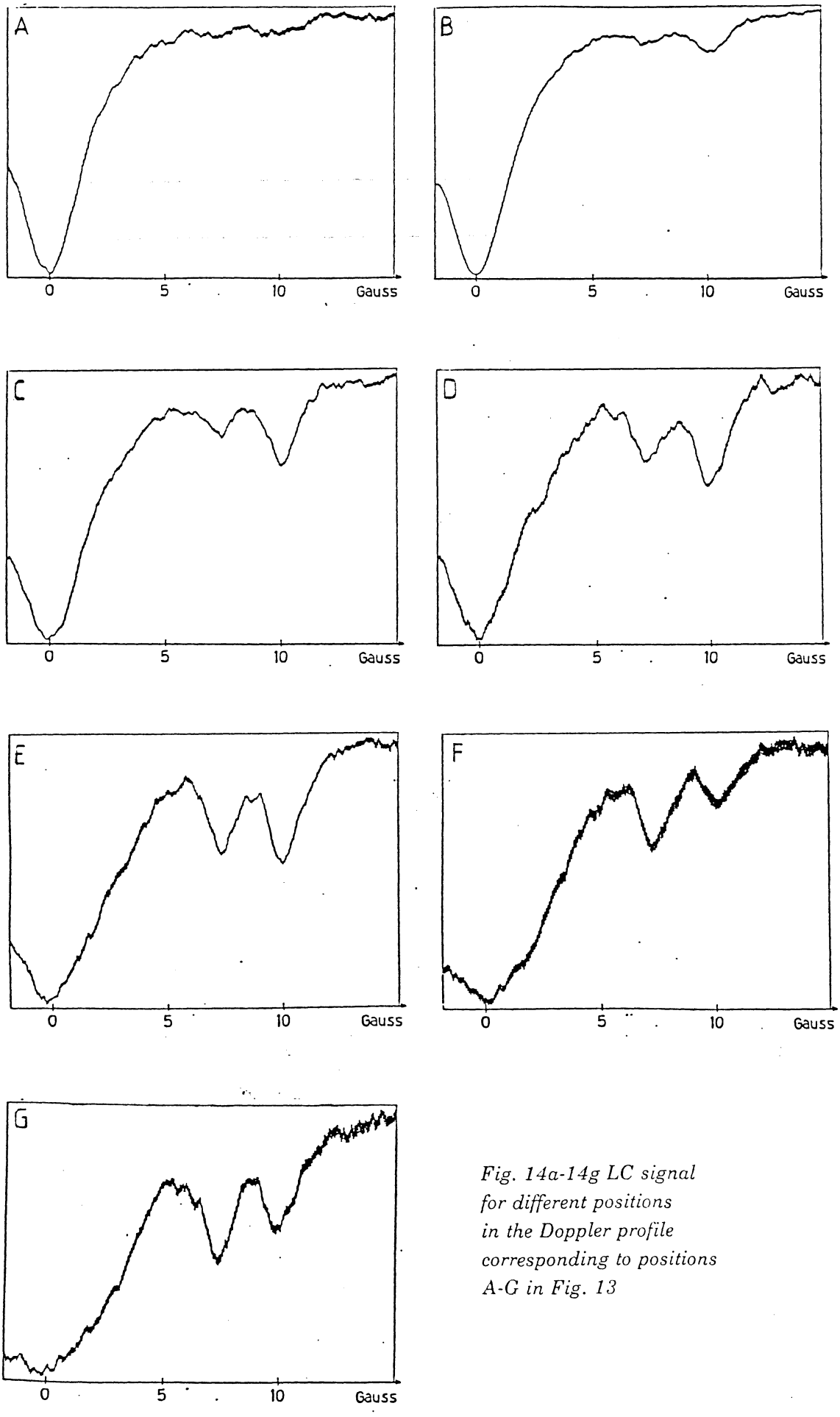

Fig. 14a-14g LC signal for different positions in the Doppler profile corresponding to positions A-G in Fig. 13

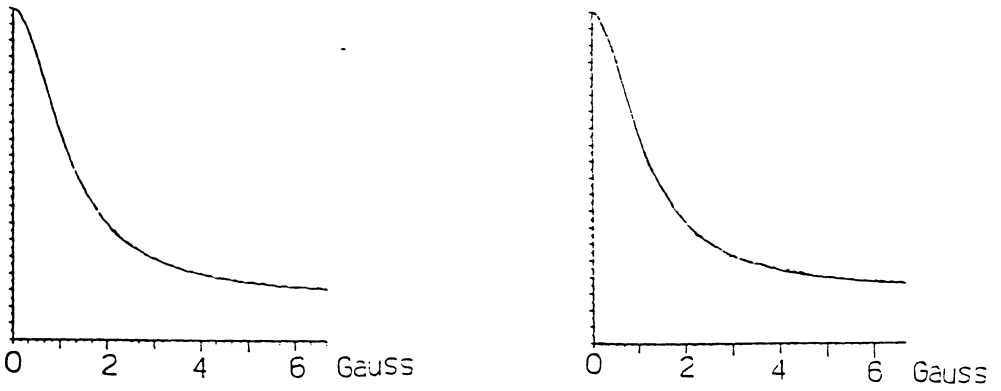

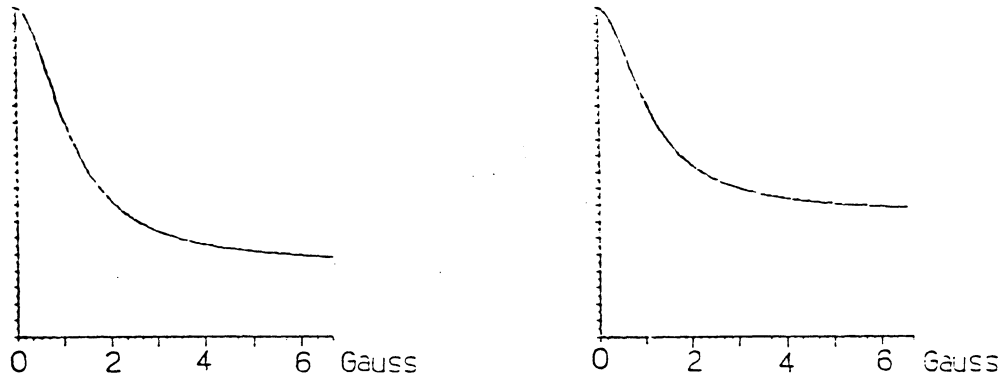

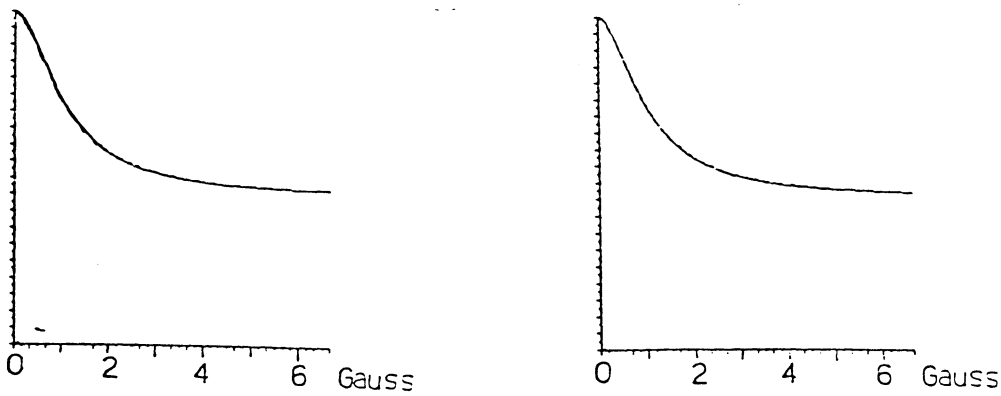

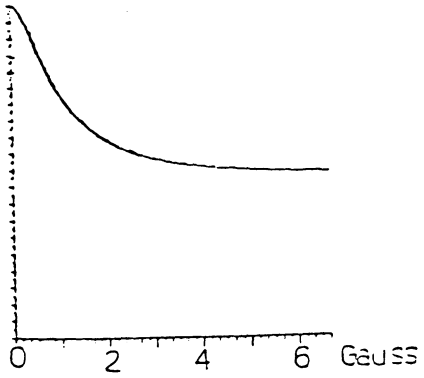

Fig. 15a-15g calculated Hanle structure corresponding to the curves in Fig. 14a-14g

Some experiments using pulsed excitation was carried out. One advantage of this techinque is the possibility of detection after the excitation source has been turned off. This technique is in this diploma work denoted as afterglow detection. Afterglow detection, eliminates the laser background and possible AC Stark effect, which can occur at high intensities. A free additional option is delayed detection which may improve the resolution further. When these experiments were carried out, no pulsed laser was available. To investigate the technique an acousto-optic modulator was inserted in the CW beam, to simulate a pulsed laser. The energy in each pulse is of course extremely small, but a repetition rate of 1MHz instead of typically 10 Hz made the experiments possible. For the pulsed experiments, further electronic units were introduced. A delay generator trigged by the control signal for the modulator opened a gate between photon counting circuits and the lock-in. The only available gate accepted positive signals only, otherwise direct input from PMT gave a better result. The problem with photon counting in a set-up as the one described, is of course the RF interaction. In our experiments this effect mainly originated from the RF lamp. To minimise the problem, amplifiers were put very close to the PMT, thus allowing a short cable. A discriminator eliminated the RF noise but unfortunately also a part of the signal. The output from the discriminator was gated to the lock-in. When the signal is put through directly from the PMT, the RF interaction is a sinus curve superimposed on the true signal. The RF frequency is high and averaged to approximately zero giving no contribution to the signal. The modified set-up is illustrated in Fig. 16.

The delayed detection experiments were carried out in the 9^2D states of ^{133}Cs. The life-time of these states are τ=208ns [20]. In the LC experiments the narrowing and the oscillations predicted by theory are evident (Fig. 17). Such oscillations can be surpressed, using apodisation [21], [22].

For the $9^2D_{5/2}$ state by the same reasons as for the $8^2D_{5/2}$ state, ODR was used. Here the signals come from different m_I -values and since they are close to each other in comparison to the Dopplerwidth the appearance of the signal is not expected to change, as the laser is tuned. The signal consist of eight peaks which are unresolved even at subnatural resolution. However the oscillations which can be seen in the flanks originate from the delayed detection (Fig. 18).

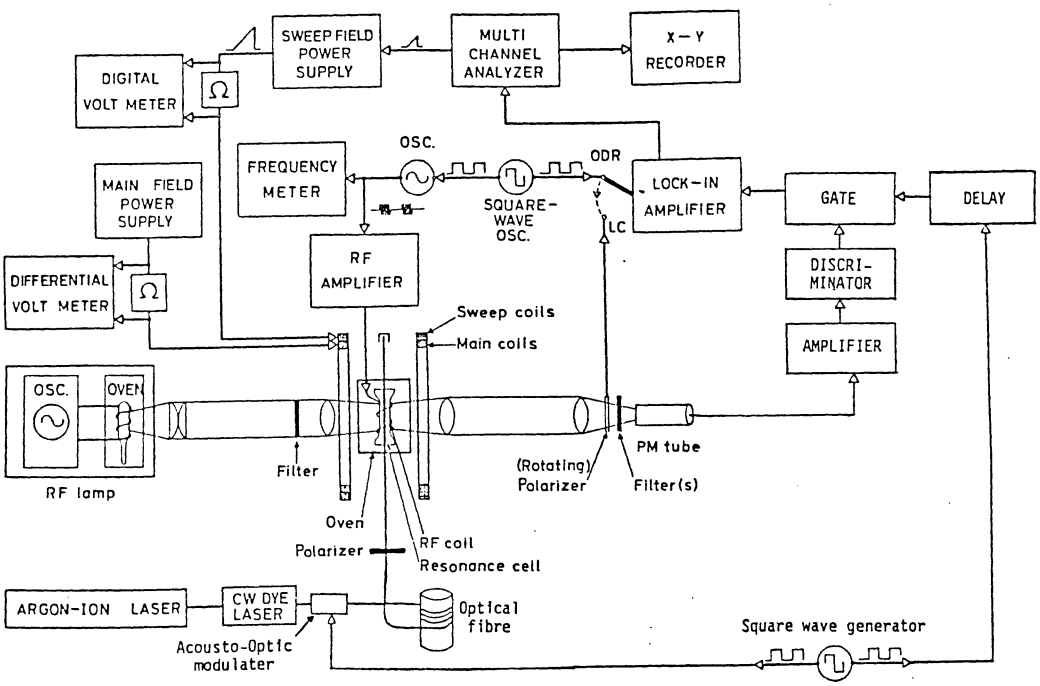

Fig.16 Experimental set-up used in pulsed excitation experiments

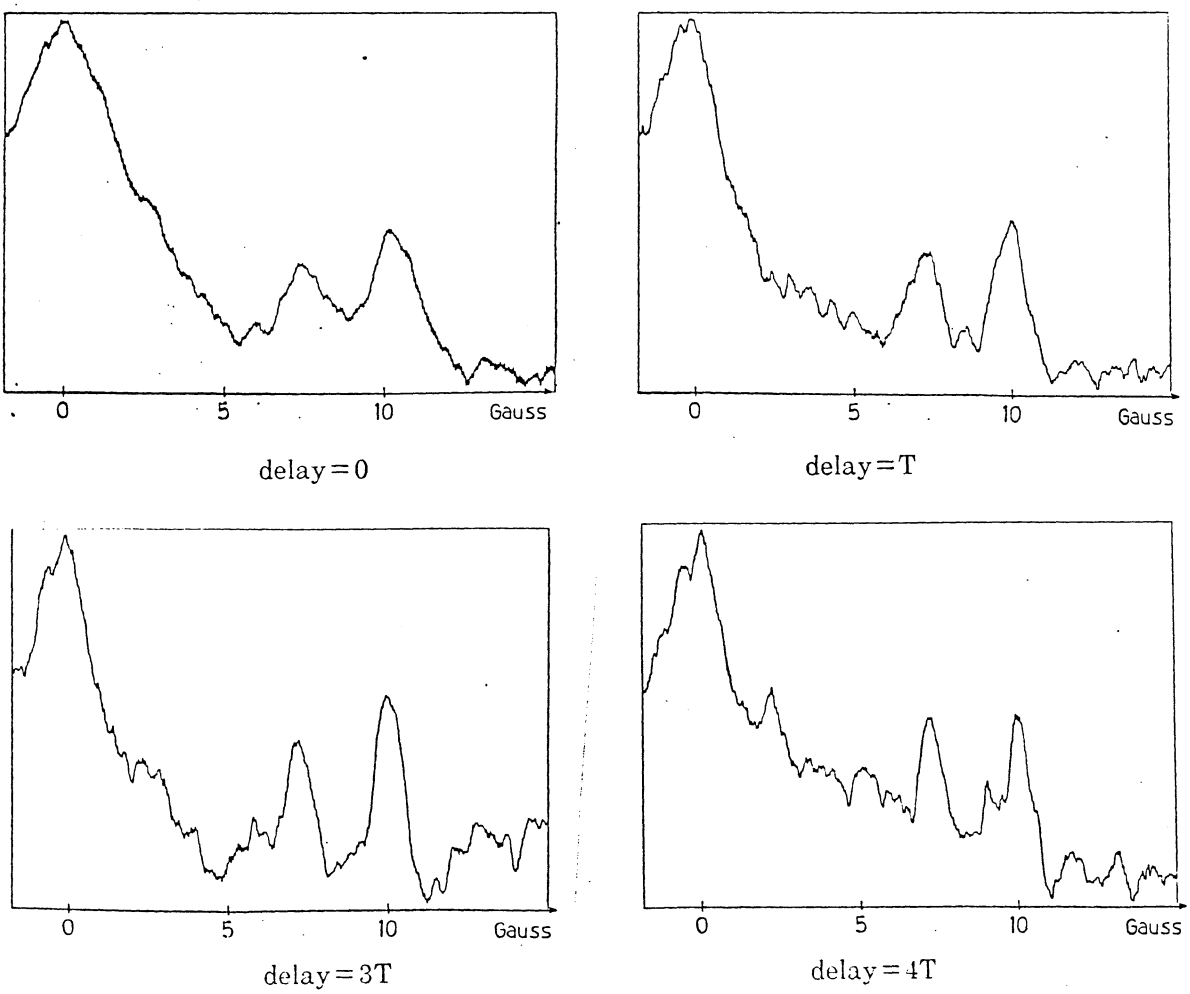

Fig. 17 Plot from LC experiment on the $9^2D_{3/2}$ level in ^{133}Cs using delayed detection.

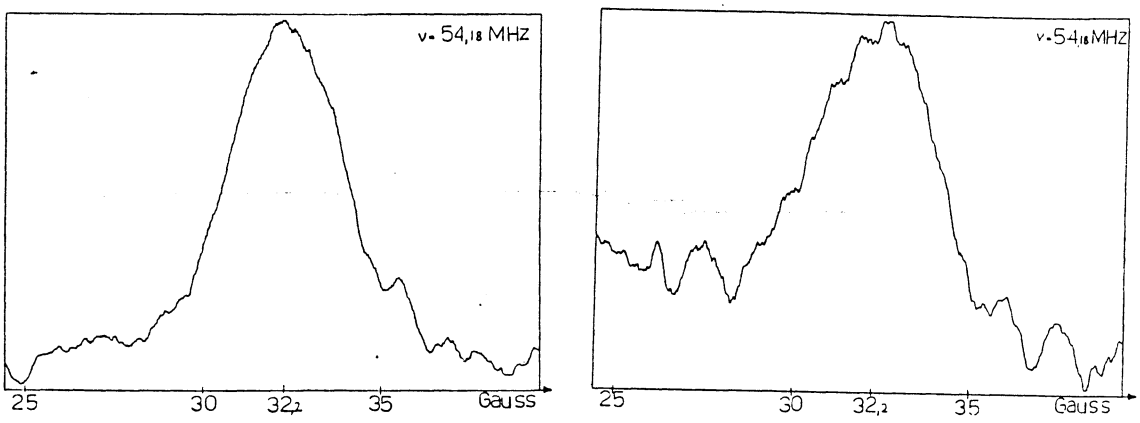

delay = 0 delay = 4T

Fig. 18 Plot from ODR experiment on the $9^2D_{3/2}$ state in ^{133}Cs using delayed detection

Computer programs

For the evaluation of experimental hyperfine structure data several programs are available. Most of these programs were developed at the Chalmers University of Technology in the sixties and seventies. The program language is FORTRAN IV. Some of these programs are described in this diploma work. Specific examples and program listings are given in a separate Appendix.

A. The Breit formula

This program simulates a level crossing experiment.

Input: Nuclear spin
Ground state atomic spin
Magnetic dipole moment of the nucleus
Isotopic abundance
For excited state:
Atomic spin
g_J,a,b-factors
Lifetime
Stark constant

Polarisation vectors for exciting and detected light.
Fixed value of electric field
Region for magnetic field
Modulation field

Result: Intensity of detected light at various fields
Plot of LC-curve
State vectors for the levels in the excited state
Energy levels for the excited state

B. Jhalf1 Jhalf2

Jhalf1 and Jhalf2 are two programs developed for J=1/2 states. They calculate the magnetic field at which RF-transitions between the (I+0.5,-I+0.5) and the (I+0.5,-I-0.5) respectively the (I+0.5,I+0.5) and the (I+0.5,I-0.5) levels occur, using the Breit-Rabi formula. (Fig.19)

Input: J,g_J,g_I
astart,aintervall,number of a-values
Hstart,Hintervall
RFstart,RFintervall,number of RF-values

Result: The magnetic field at different frequencies and a-values

The magnetic field must be known to have its values between Hstart and Hstart+Hintervall·200
The accuracy is Hintervall

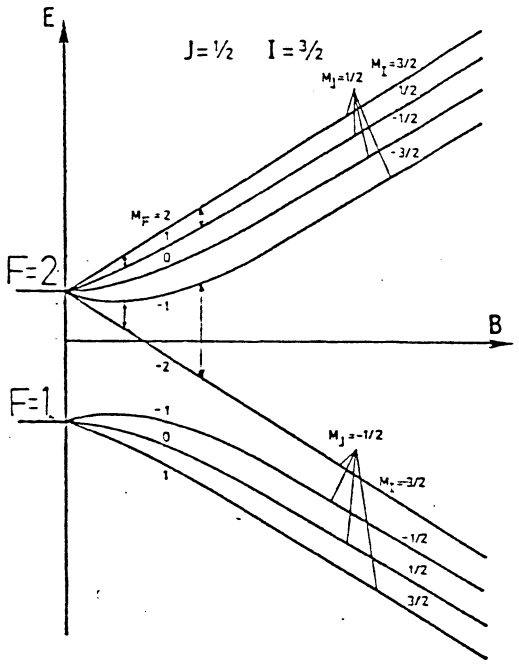

Fig. 19 An example of a J=1/2 system

C. Resfrop

This program calculates the resonance frequencies for transitions between two levels.

Input: J,I
F,m for the two levels
Hintervall,Hmax
Accuracy,Maximum number of iterations for each frequency

Result: Frequencies (MHz)
Hintervall /(Frequency-last frequency)
Energy for the two levels (MHz from centre of gravity)
Accuracy (expressed in number of units wrong in last decimal)

D. Hanle Effect Program

This program simulates a level crossing experiment using a simple Zeeman model. The results are obviously valid only in this region and thus only the Hanle signal can be studied. It is however possible to use different illumination profiles, and to see their effect on the Hanle signal.

Input: Nuclear spin
Total angular momentum in the
Ground state
Excited state
Final state
Illumination profile between hyperfine levels in the ground state and the excited state.

Result: Plot of Hanle curve.

Discussion

To further develop the techniques described in this diploma work other experiments will be carried out. A pulsed Nd YAG-laser pumping a dye laser will be used. Free atoms will be produced in an atomic beam apparatus. This discussion will mainly concern these experiments.

One difficulty in pulsed laser excitation is that the energy fluctuates much between different laser shots. To overcome this a two detector set-up will be used. By monitioring a dimensionless quanty unknown factors will disappear. This dimensionless quantity could for instance be chosen as

$$Q1 = \frac{I(\pi) - I(\sigma)}{I(\pi) + I(\sigma)} \qquad \text{or} \qquad Q2 = \frac{I(\pi)}{I(\sigma)}$$

A similar two detector set-up in ODR was in fact used by Brossel and Bitter in their first experiment [2].

The arrangement could in principle have been tested using the modulated CW-laser. The normalisation would not have been successful since the signal in each pulse is very small. The average number of photons per pulse was less than one. Using the Nd YAG-system large amounts of energy will be deposited at a repetition rate of typically 10 Hz. There will be a large number of photons and the idea will be practically applicable.

In this diploma work pulsed excitation was used in combination with lock-in detection. To make this work the repetition rate must be much higher than the lock-in frequency. This is not possible using a 10 Hz laser. Instead boxcar integration is expected to be a good alternative. (Fig. 20).

The available (EG&G Type 162) boxcar averager has two inputs A and B and is able to create the quantity A/B. Keeping the time window at a constant position the output capacitance will get an increase of voltage proportional to the total intensity of the light in the time set by the boxcar time window. Reading out the voltage over the capacitance every fifth laser pulse, assuming a laser repetition rate of 10 Hz, a five minute sweep is demanded to get a resolution of 600 points. Another possible way is to use a unit forming the quotient Q1 for every shot and use a signal averager for improving the (S/N) ratio.

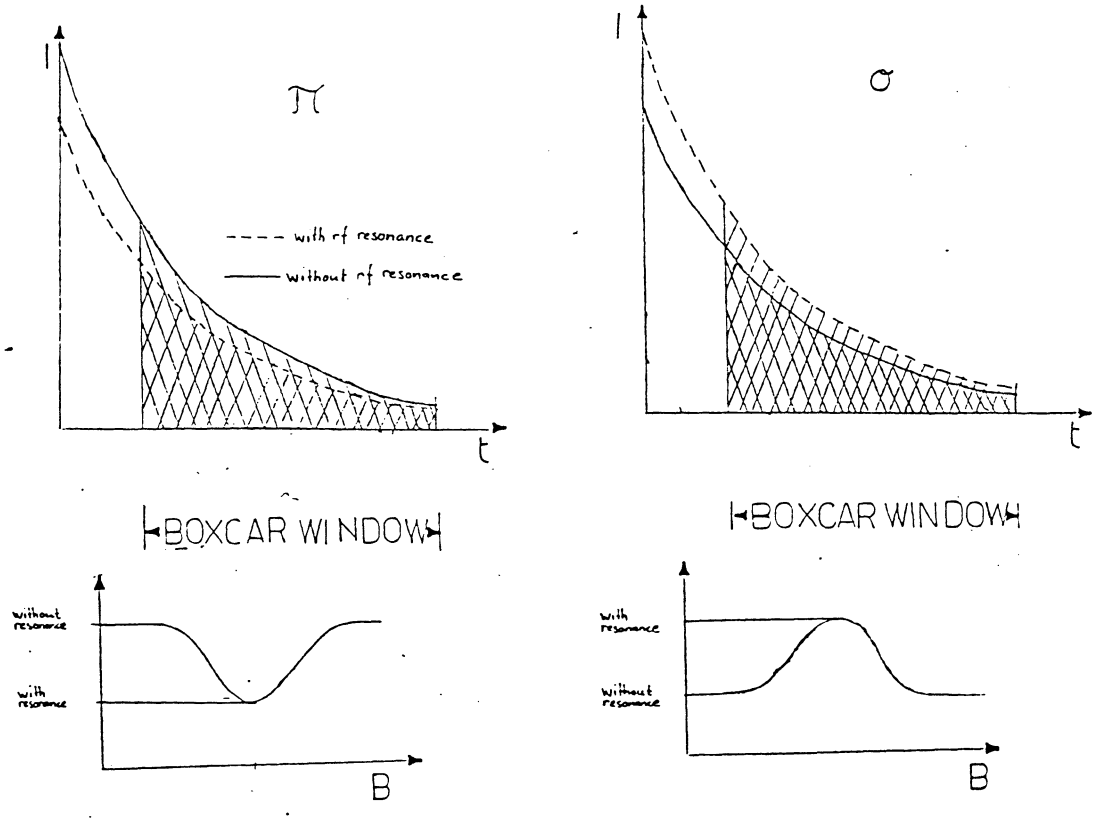

Fig. 20 Illustration of pulsed ODR experiment.

Appendix 1 The Breit formula.

This derrivation is the one given by Franken [6], with additional comments, and the correct sign in the denominator. This descripancy in the Breit formula was not noted until 1968, when Khadjavi et al [23] and Stroke et al [24] pointed it out.

In this diploma work, laser excitation was used. The theory of coherent light excitation in combination with resonance scattering is complex. In this derrivation incoherent, "white" light originating from source atoms of decay rate γ is assumed. The decay rate of the sample atoms is denoted by Γ.

At t=0 the sample atom is in a ground state u_m and the source atom is excited. The state of the sample atom is described by

$$\Psi = u \qquad t<0 \tag{A1.1}$$

$$\Psi = \sum_{\mu}^{m} a_{\mu}(t)u_{\mu} + b_m(t)u_m \qquad t>=0 \tag{A1.2}$$

The functions u_n are time independant wave-functions for the unperturbed atom.

The sample atom experience an electric field $\underline{E}$, for T>=0 due to the decay of the source atom.

$$\underline{E} = \underline{f} \cdot E_0 \cos\omega t \cdot e^{-\gamma t} = \underline{f} \cdot E_0 \cdot e^{-i\omega t/2 - \gamma t} \tag{A1.3}$$

$\underline{f}$ is the polarization vector and ω is the central angular frequency.

The Hamiltonian is written as

$$H = H_0 + H' \tag{A1.4}$$

where H_0 is the Hamiltonian for the atomic system, when the electromagnetic pertubation is not present. This pertubation is

$$H' = e \cdot \underline{E} . \underline{r} \tag{A1.5}$$

Combining (A1.2) with the time-dependant Schrödinger equation give

$$\frac{d}{dt}\left(\sum_{\mu'} a_{\mu'}(t)u_{\mu'} + b_{m'}(t)u_{m'}\right) = \frac{1}{i\hbar}\left[(H_0+H')\left(\sum_{\mu'} a_{\mu'}(t)u_{\mu'} + b_{m'}(t)u_{m'}\right)\right] \tag{A1.6}$$

multiplication with u_μ and integration over space give

$$\dot{a}_\mu = -i\omega a_\mu + \frac{1}{i\hbar}\sum_{\mu'} H'_{\mu\mu'} a_{\mu'}(t) + \frac{1}{i\hbar} H'_{\mu m} b_m(t) - \frac{1}{2}\Gamma a_\mu \tag{A1.7}$$

The last term describe the radiation damping of the excited states.

If the two excited states have the same electronic momentum (i.e the same L-value), such transitions are not possible and the Σ -term disappear. Otherwise, its contribution is negligable.

In this first-order pertubation calculation, $b_m(t)=1$.

After these simplifications the Schrödinger equation yield

$$\dot{a}_\mu = B_\mu e^{-i\omega t-\gamma t/2} - \left(\frac{1}{2}\Gamma + i\omega\right)a_\mu \qquad (A1.8)$$

$$B_\mu = (eE_0/2i\hbar) \cdot \langle\mu|\underline{f}.\underline{r}|m\rangle \qquad (A1.9)$$

Solving (A1.7) is done by standard methods. Multiplying by $e^{\Gamma/2+i\omega}$ and rewriting the equation as the derrivata of a product, give as the boundary condition $a_\mu=0$ at $t=0$ is taken.

$$a_\mu(t) = B_\mu \cdot e^{-(\Gamma/2+i\omega)t} \cdot \left[\frac{e^{i(\omega_\mu-\omega)} - 1}{i(\omega_\mu-\omega) - \lambda}\right] \qquad (A1.10)$$

$\lambda = 1/2(\gamma-\Gamma)$

Due to spontaneous emission, photons are emitted. The rate at which photons of polarisation $\underline{g}$ is emitted is given by

$$S(\underline{f},\underline{g},t) = \sum_{m'} \left| \sum_{\mu'} a_{\mu'}(t) \cdot \langle u_{\mu'}|\underline{g}.\underline{r}|u_{m'}\rangle \right|^2 \qquad (A1.11)$$

The rate $S(\underline{f},\underline{g})$ at which photons of polarization $\underline{f}$ are absorbed and those of polarization $\underline{g}$ are re-emitted can be arrived at, by integration over time and frequiency. The time between flourocense events is assumed to be much larger as the flouroscence cykle time. Furthermore "white" excitation is assumed. Integration should then be carried out from $t=0$ to ∞ and over all frequiencies. The time integral is straight-forward, but to solve the frequency integral residy-calculus is demanded. All ground states should be taken into consideration, and a summation over theese is required. As the summation is done, the following expression is obtained

$$S = C \cdot \sum_{\mu\mu' mm'} f_{m\mu'} \cdot f_{\mu m} \cdot g_{m'\mu} g_{\mu' m'} \cdot \int dt \int d\omega \frac{e^{-i\omega_{\mu\mu'}t} - \Gamma t}{[(\omega_\mu-\omega)+i\lambda]\cdot[(\omega_{\mu'}-\omega)-i\lambda]} \cdot$$

$$\cdot \left[e^{i\omega_{\mu\mu'}t-2\lambda t} - e^{i(\omega_\mu-\omega)t-\lambda t} - e^{-i(\omega_{\mu'}-\omega)t-\lambda t} + 1 \right] \qquad (A1.12)$$

As the integrations are carried out the Breit formula is arrived at.

$$S = C \cdot \sum_{\mu\mu' mm'} f_{m\mu'} \cdot f_{\mu m} \cdot g_{m'\mu} \cdot g_{\mu' m'} \cdot \frac{1}{\Gamma + i\omega_{\mu\mu'}} \qquad \text{(A1.13)}$$

Appendix 2 LC lineshapes

As stated in [14]

$$S = C \cdot \sum_{MM'mm'} \frac{\mathrm{Re}\,(K_{\mu\mu'}) + 2\cdot\pi\cdot\tau\cdot\nu_{\mu\mu'}\cdot \mathrm{Im}\,(K_{\mu\mu'})}{1 + 4\cdot\pi^2\cdot\tau^2\cdot\nu_{\mu\mu'}} \qquad \text{(A2.1)}$$

$K_{\mu\mu'}$ is defined as

$$K_{\mu\mu'} = \sum_{mm'} f_{\mu m}\cdot f_{m\mu'}\cdot g_{\mu' m'}\cdot g_{m'\mu} \qquad \text{(A2.2)}$$

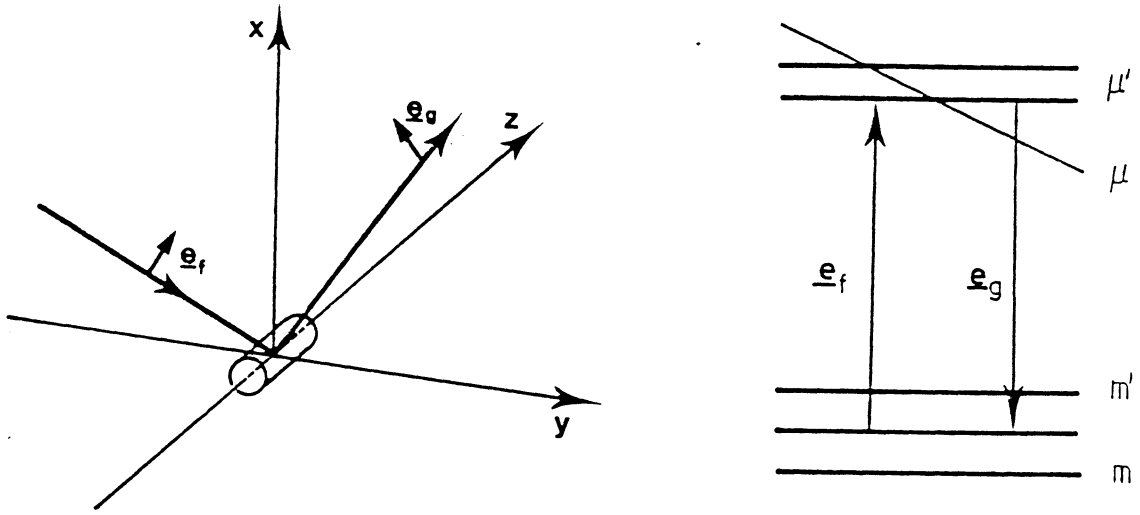

Fig. A2 Resonance scattering

The coordinate system is given by Fig. A2. The magnetic field is parallel to the z-axes.

Excitation polarisation parallel to y-axes

$$f_{\mu m} = \langle\mu|\underline{e}_y.\underline{r}|m\rangle$$
$$= \langle\mu|\ y\ |m\rangle = (1/2i)\cdot\langle\mu|x_+ - x_-|m\rangle$$
$$= 0,\ |\mu - m| \neq 1 \qquad \text{(A2.3)}$$

$f_{\mu m}$ is imaginary

$$f_{m\mu'} = \langle m|\underline{e}_y.\underline{r}|\mu'\rangle$$
$$= \langle m|y|\mu'\rangle = (1/2i)\cdot\langle m|x_+ - x_-|\mu'\rangle$$
$$= 0,\ |\mu' - m| \neq 1 \qquad \text{(A2.4)}$$

$f_{m\mu'}$ is imaginary

$f_{\mu m}\cdot f_{m\mu'}$ is a real $\neq 0$ when $|\mu - \mu'| = 0$ or 2

With this set-up only $\Delta\mu=2$ crossings can be studied since $\mu=0$ levels obey the non-crossing rule.

Detection polarisation parallel to y-axis

$$g_{\mu'm'}=\langle\mu'|\underline{e}_y.\underline{r}|m'\rangle$$
$$=\langle\mu'|y|m'\rangle=(1/2i)\cdot\langle\mu'|x_+ - x_-|m'\rangle$$
$$=0,\ |\mu'-m'| <> 1 \qquad \text{(A2.5)}$$

$g_{\mu'm'}$ is imaginary

$$g_{m'\mu}=\langle m'|\underline{e}_y.\underline{r}|\mu\rangle$$
$$=\langle m'|y|\mu\rangle=(1/2i)\cdot\langle m'|x_+ - x_-|\mu\rangle$$
$$=0,\ |\mu-m'| <> 1 \qquad \text{(A2.6)}$$

$g_{m'\mu}$ is imaginary

$g_{\mu'm'}\cdot g_{m'\mu}$ is real and none zero for $\Delta\mu=2$ crossings

Thus $K_{\mu\mu'}$ is real and a Lorenz shaped signal is expected

Detection polarisation parallel to x-axis

$$g_{\mu'm'}=\langle\mu'|\underline{e}_x.\underline{r}|m'\rangle$$
$$=\langle\mu'|x|m'\rangle=(1/2)\cdot\langle\mu'|x_+ + x_-|m'\rangle$$
$$=0,\ |\mu'-m'| <> 1 \qquad \text{(A2.7)}$$

$g_{\mu'm'}$ is real

$$g_{m'\mu}=\langle m'|\underline{e}_x.\underline{r}|\mu\rangle$$
$$=\langle m'|x|\mu\rangle=(1/2)\cdot\langle m'|x_+ + x_-|\mu\rangle$$
$$=0,\ |\mu-m'| <> 1 \qquad \text{(A2.8)}$$

$g_{m'\mu}$ is real

$g_{\mu'm'}\cdot g_{m'\mu}$ is real and none zero for $\Delta\mu=2$ crossings

Thus $K_{\mu\mu'}$ is real and a Lorenz shaped signal is expected

Detection polarisation 45 degrees to x- and y-axis

$$g_{\mu'm'}=1/\sqrt{2}\cdot\langle\mu'|(\underline{e}_x + \underline{e}_y).\underline{r}|m'\rangle$$

$$
\begin{aligned}
&= 1/\sqrt{2} \cdot \langle \mu' | x + y | m' \rangle \\
&= (1/(2 \cdot \sqrt{2})) \cdot \langle \mu' | (1-i) \cdot x_+ + (1+i) \cdot x_- | m' \rangle \\
&= (1/(2 \cdot \sqrt{2})) \cdot [\langle \mu' | x_+ | m' \rangle + \langle \mu' | x_- | m' \rangle - \\
&\quad i \cdot \langle \mu' | x_+ | m' \rangle + i \cdot \langle \mu' | x_- | m' \rangle] \\
&= 0, \quad |\mu' - m'| \neq 1
\end{aligned} \tag{A2.9}
$$

$g_{\mu' m'}$ is complex

$$
\begin{aligned}
g_{m' \mu} &= 1/\sqrt{2} \cdot \langle m' | (\underline{e}_x + \underline{e}_y) . \underline{r} | \mu \rangle \\
&= 1/\sqrt{2} \cdot \langle m' | x + y | \mu' \rangle \\
&= (1/(2 \cdot \sqrt{2})) \cdot \langle m' | (1-i) \cdot x_+ + (1+i) \cdot x_- | \mu \rangle \\
&= 1/(2 \cdot \sqrt{2}) \cdot [\langle m' | x_+ | \mu \rangle + \langle m' | x_- | \mu \rangle - \\
&\quad i \cdot \langle m' | x_+ | \mu \rangle + i \cdot \langle m' | x_- | \mu \rangle] \\
&= 0, \quad |\mu - m'| \neq 1
\end{aligned} \tag{A2.10}
$$

$g_{m' \mu}$ is complex

$$
\begin{aligned}
g_{\mu' m'} \cdot g_{m' \mu} &= 2 \cdot i \cdot \langle \mu' | x_+ | m' \rangle \cdot \langle m' | x_+ | \mu \rangle \qquad (\mu' - \mu) = 2 \\
&\quad 2 \cdot i \cdot \langle \mu' | x_- | m' \rangle \cdot \langle m' | x_- | \mu \rangle \qquad (\mu' - \mu) = -2
\end{aligned} \tag{A2.11}
$$

$g_{\mu' m'} \cdot g_{m' \mu}$ is imaginary and none zero for $\Delta\mu = 2$ crossings

Thus $K_{\mu\mu'}$ is imaginary and a dispersion shaped signal is expected

Appendix 3 Cell manufacturing

A number of resonance and lamp cells were manufactured in connection to this work. Some of the practical aspects of cell manufacturing will here be described.

The kind of glass used was Pyrex due to a low temperature expansion coefficient. A pumping bench originating from Chalmers University of Technology was used. The glass constructions was manufactured by the glass blower at the Department of Chemistry, Lund.

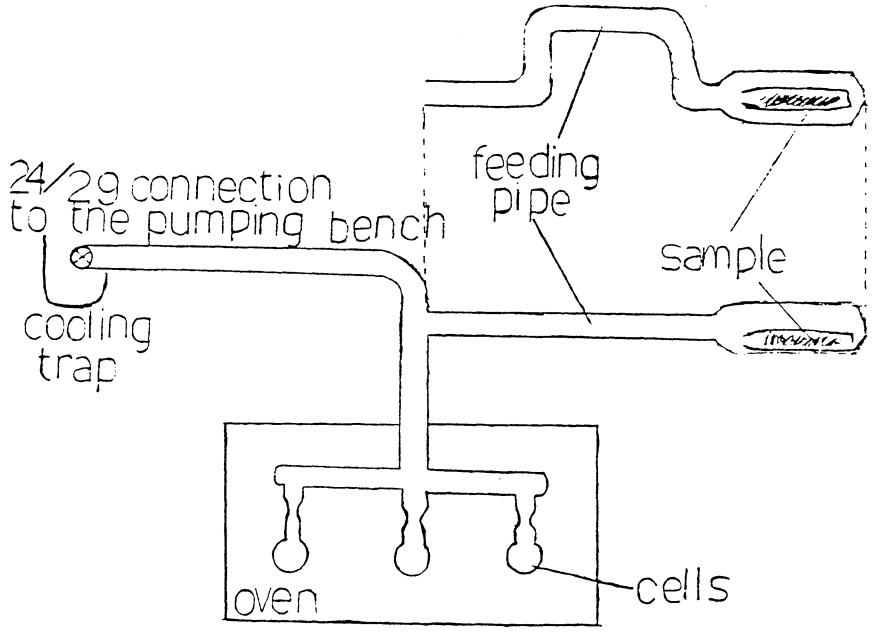

Fig. A3 Set-up

The principle is to distil the sample so that all impurities of higher boiling temperatures are left behind. Hence it is important to make sure that the sample is moved in gas phase.

Usually the sample is contained in an ampulla. Then at the end of the feeding pipe there are two layers of glass and boiling can easily occur. To prevent the sample from reaching the cells in liquid phase the feeding pipe should be curved. To make it easier for the sample to leave the ampulla, the end of the feeding pipe could be constructed to lean a bit.

A procedure for cell manufacturing.

1 After receiving the glass construction from the glass blower one should make sure that it does not leak. Place the construction in the pump site, plug the rear end by a rubber stop and start pumping. Leaks can easily be detected using a Tesla generator. At the leaks a characteristic intense white light occurs.

2 The ampulla should now be broken. First make sure that the metal is at the bottom, otherwise there is a risk that the narrow upper part will be jammed with oxides. This can be taken care of by melting the metal with the ampulla in an upright position. An ordinary hair-drier is sufficient for melting Rb and Cs.

3 Load the sample. Connect a glass rod to the rear part of the feeding pipe using a gas torch burner. Heat the feeding pipe at the rear and two or three centimetres in. When the glass is soft, twist the rod so that the end of the pipe is melted together. Start pumping when the glass is hardened. To reduce the tensions in the glass, it should be cooled down slowly. Turn the oxygen off and cool the hot end off with the flame.

4 To get rid of impurities contained in the glass the cells should be baked for about 10-12 hours. By then the pressure ought to have reached below 10^{-6}. Suitable temperatures are for Pyrex 400°C and for quarts 800° C.

5 Remove the oven. Let the cells cool down. If this is not done and boiling occur above the cells the sample may boil up and down contaminating the cells.

6 Start heating carefully, using a gas torch burner. To make it easier to move the sample forward, the feeding pipe can be melted off as the sample is moved. Move the desired amount into the cells.

7 Set up the cooling trap with liquid nitrogen.

8 To melt the cells off one must make sure that the constriction is heated from all sides. At first the heating should be careful. After a short while one can let the burner close in. To feel when the melting starts, pull the cell gently. When this occours it should be pulled in a slow, even pace. The end collapses under the vacuum and is melted together. Now close in further and heat it off from one side. Melt the glass thread down with the burner. As in point 3 the cooling down should be slow. This applies to both the end of the cell and the rest of the construction.

References

1. Kastler A., Brossel J., Compt Rend. 229, 1213 (1949)
2. Brossel J., Bitter F., Phys. Rev. 86, 368 (1952)
3. Breit G., Rev. Mod. Phys. 5, 91 (1933)
4. Hanle W., Z. Physic 30, 93 (1924); Erg. Ex. Naturwiss. 4, (1925)
5. Colgrove F.D., Franken P.A., Lewis R.R., Sands R.H., Phys. Rev. Lett. 3, 420 (1959)
6. Franken P.A., Interference Effects in the Resonance Flourescence of "Crossed" Excited States, Phys. Rev. 121, 508 (1961)
7. Demtroder W., Laser Spectroscopy, Springer, Heidelberg (1981)
8. Majorana E., Nouvo Cimento 9, 43 (1932)
9. Rabi I.I., Phys. Rev. 51, 652 (1932)
10. Cagnac, Pebay-Peroula J.-C., Modern Atomic Physics, Quantum Theory and its Applications, The Macmillan Press (1975)
11. Ma, Mertens, Putlitz, Schutte, Linienform von Doppel-resonanzsignalen bei zeitlich aufgeloster Beobachtung der zerfallenden Atomzustande, Z. Phys. 208, 352 (1968)
12. O' Brien P.O., Meystre P., Walther H., Subnatural linewidths in atomic spectroscopy, Advances in Atomic and Molecular Physics, vol. 21 (Academic press, Orlando 1985)
13. Svanberg S., Tsekeris P., Hyperfine-structure investigation of highly excited D levels in Rb and Cs using a cw tunable dye laser in a two step excitation Scheme, Phys. Rev. A 11, 4 (1975)
14. Svanberg S., in Atom och Molekylspektroskopi, Sigmatryck, Lund
15. Copley G., Kibble B.P., Series G.W., J. Phys. B 1, 724 (1968)
16. Schenk P., Hilborn R.C., Metcalf H., Time Resolved Flourescence from Ba and Ca Excited by a Pulsed Tunable Dye Laser, Phys. Rev. Lett. 31, 4 (1973)
17. Condon, Shortley, in Theory of Atomic Spectra
18. Svanberg S., Belin G., Z. Phys. 251, 1
19. Svanberg S., Physica Scripta 5, 1-2 (1972)
20. Deech J.S., Luypaert R. and Series G.W. J. Phys. B 8, 1406 (1975)
21. Figger H., Walther H., Z. Phys. 267, 1 (1974)
22. Deech J.S., Hannaford P., Series G.W., J. Phys. B 7, 1131 (1974)
22. Khadjavi A., Allen L. and Happer. W., Phys. Rev. 167, 128 (1968)
23. Stroke H.H., Fulop G., Kleipner S. and Redi O., Phys. Rev. Lett. 21, 61 (1968)